

· 综述与进展 ·

## 俯冲带中石墨质碳的研究进展

胡 焖, 张立飞

(北京大学 造山带与地壳演化教育部重点实验室, 北京 100871)

**摘要:** 自然界中, 石墨质碳可以稳定存在于沉积岩、岩浆岩和变质岩中, 由有机质或无机碳酸盐转变而来。随着对俯冲带碳循环研究的不断深入, 通常作为副矿物产出在变质岩中的石墨质碳也引起了广泛的关注。相比于碳酸盐矿物和含碳流体, 石墨质碳因其低溶解性、低移动性常作为碳汇稳定存在于俯冲带中。然而, 在一些特殊的地质条件下(例如流体出现的开放体系中), 石墨质碳不再稳定, 它会变得活跃并发生迁移。因此, 石墨质碳也是俯冲带碳循环研究中的关键载体。本文在综述前人研究成果的基础上, 总结了俯冲带中石墨质碳的性质、来源、形成和分解过程, 并重点介绍了俯冲带中非生物成因石墨的形成机制、石墨质碳的稳定性以及石墨质碳的释放, 全面探讨了石墨质碳在俯冲带碳循环中的重要意义。俯冲带中石墨质碳的成因机制主要有3种: 生物有机质石墨化、饱和含碳流体沉淀、碳酸盐矿物的还原反应。俯冲带中石墨质碳可通过分解脱气和溶解的方式释放。俯冲作用和风化侵蚀是石墨质碳全球循环的两个主要过程, 其中俯冲作用对石墨质碳的地球内部循环影响较大。

**关键词:** 石墨; 俯冲带; 非生物成因; 变质岩; 碳循环

中图分类号: P542.5; P578.1<sup>+6</sup>

文献标识码: A

文章编号: 1000-6524(2021)04-0764-14

## Progress of research on graphitic carbon in subduction zones

HU Han and ZHANG Li-fei

(Key Laboratory of Orogenic Belts and Crustal Evolution, MOE, Peking University, Beijing 100871, China)

**Abstract:** Graphitic carbon is mainly transformed from organic compounds or carbonate minerals in nature, and can exist stably in sedimentary rocks, magmatic rocks and metamorphic rocks. With the development of research on the carbon cycle in subduction zones, graphitic carbon, which usually occurs as accessory mineral in metamorphic rocks, has increasingly attracted attention. Graphitic carbon can be stable in subduction zones as carbon sinks due to its low solubility with respect to carbonate and the low mobility with respect to carbonic fluids. However, graphitic carbon can be reactive under some special geological conditions (e.g., with the presence of aqueous fluids in open systems), and becomes active and migrates. Therefore, graphitic carbon is one of the key subjects to trace carbon cycle in subduction zones. Based on previous studies, this paper provides an overview of the properties, formation, and decomposition of graphitic carbon in subduction zones, and comprehensively discusses the abiogenic genesis, the stability and the release of them, which can be a key participant in the carbon cycle in subduction zones. There are three main genetics mechanisms of graphitic carbon in subduction zones: graphitization of biological organic matter, precipitation of saturated carbonic fluid, and reduction of carbonate minerals. Graphitic carbon in subduction zones can be released through degassing and fluid-mediated dissolution. Subduction and weathering erosion are the two main processes in the global cycle of graphitic carbon, with subduction having a greater impact on

收稿日期: 2020-12-24; 接受日期: 2021-05-19; 编辑: 尹淑萍

基金项目: 国家重点研发项目(2019YFA0708501)

作者简介: 胡 焖(1994- ), 女, 博士研究生, 变质地质学专业, E-mail: huhan1@pku.edu.cn; 通讯作者: 张立飞(1963- ), 男, 理学博士, 教授, 主要从事变质地质学研究, E-mail: lfzhang@pku.edu.cn。

the internal circulation of graphitic carbon.

**Key words:** graphite; subduction zones; abiotic synthesis; metamorphic rocks; carbon cycle

**Fund support:** National Basic Research Program of China (2019YFA0708501)

地壳碳的俯冲在全球碳循环中起着核心作用,碳酸盐矿物和石墨质碳(graphitic carbon)是俯冲板片中碳的主要存储媒介(Hayes and Waldbauer, 2006; Plank, 2014)。石墨质碳通常指所有具有由芳族碳原子组成的骨架的多尺度组织的固体含碳化合物(Buseck and Beyssac, 2014)。过去几十年来,前人关于碳酸盐矿物的脱碳机制(例如脱碳反应、熔融反应和碳酸盐溶解反应)已经做了大量的研究(Gorman *et al.*, 2006; Ague and Nicolsescu, 2014; Cook-Kollars *et al.*, 2014; Facq *et al.*, 2014; Kelenmen and Manning, 2015; Poli, 2015)。尽管石墨质碳是俯冲带有机碳(organic carbon, 沉积岩中含有的与有机质有关的碳,包含石墨质碳和碳氢化合物)的主要输入载体,但其对深部碳通量的贡献却鲜为人知(Hayes and Waldbauer, 2006; Beyssac and Rumble, 2014; Plank, 2014)。

在俯冲作用的早期阶段( $<300^{\circ}\text{C}$ ),石墨质碳中碳的释放过程会导致包括热生烃(thermogenic hydrocarbons)和 $\text{CO}_2$ 在内的含碳化合物的释放(Mullis *et al.*, 1994; Tarantola *et al.*, 2007)。随着俯冲过程中温度的升高,含碳物质通过一系列无序石墨质碳的中间阶段逐渐转变为石墨(Buseck and Beyssac, 2014)。在俯冲带条件下,通常认为石墨质碳的移动性比碳酸盐矿物的移动性差(Frost, 1979; Connolly, 1995; Caciagli and Manning, 2003; Frezzotti *et al.*, 2011)。其次,由于石墨质碳在氧化地质流体中具有高缓冲潜力(石墨可以与氧化性的含碳流体共存)(Hermann *et al.*, 2006; Duncan and Dasgupta, 2017),因此即使在高温条件下,石墨质碳(尤其是结晶的石墨)也可大量保留在俯冲带岩石中。

目前,尽管对俯冲带中石墨质碳的研究工作已经陆续开展(Galvez *et al.*, 2013a, 2013b; Tumiati *et al.*, 2017; Vitale Brovarone *et al.*, 2020; Zhu *et al.*, 2020),但是对于俯冲带中石墨质碳的成因机制研究,尤其是非生物成因的石墨质碳,关注较少。本文在总结前人研究成果的基础上,介绍了俯冲带中石墨质碳的形成、分解及转化过程,归纳总结了俯冲带中石墨质碳的形成机制及其释放,并对石墨质碳在俯冲带碳循环中的意义进行了深入探讨。

## 1 石墨质碳的特征

石墨质碳具有多种结构和化学组成,包含从无定型碳(amorphous carbon, 指石墨化程度很低,近似非晶态的含碳物质,其C/H原子比大于10,如煤烟、低级煤),到具有无数个涡轮层状结构的变质岩中的碳质物(carbonaceous matter),再到高度结晶的石墨(graphite, 分子式为C)(Franklin, 1951; Buseck and Beyssac, 2014)(图1)。本文不详细区分这三者,统称为石墨质碳。

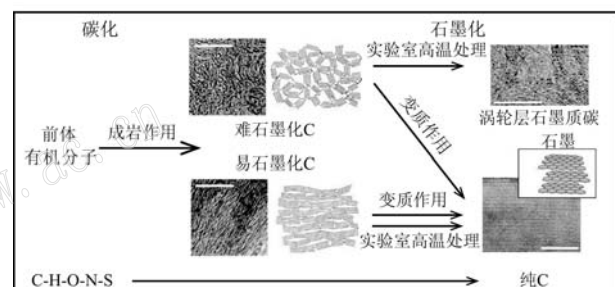


图1 有机化合物通过碳化和石墨化阶段转化为石墨的示意图[据Buseck and Beyssac(2014)修改]

Fig. 1 Schematic diagram of the transformation of organic compounds into graphite through the carbonization and graphitization stages (modified after Buseck and Beyssac, 2014)

难石墨化碳在实验室高温处理(高达 $3\,000^{\circ}\text{C}$ )后仍保持其较差的堆积顺序,但在高级变质作用下( $t>700^{\circ}\text{C}$ )可转化为石墨。TEM图像的标尺为10 nm。易石墨化和难石墨化碳的结构模型来自Franklin(1951)

Nongraphitizable carbon retains its poorly ordered stacking after laboratory heat treatment (up to  $3\,000^{\circ}\text{C}$ ), whereas it transforms into graphite under high-grade metamorphism ( $t>700^{\circ}\text{C}$ ). Scale bar for the TEM images is 10 nm. Structural models of graphitizable and nongraphitizable carbon are from Franklin (1951)

石墨质碳作为特征矿物或副矿物广泛产出在经历不同温压变质作用的岩石中。变质岩中石墨最早由Miyashiro(1964)报道,随后在很多变质沉积岩中都有石墨的发现(Landis, 1971; Diessel and Offler 1975; Berglund and Touret 1976; Black, 1977)。在许多前寒武纪高级变质地层中,石墨质碳表现为层状或脉状富集成矿,例如我国华北克拉通孔兹岩带(Yang *et al.*, 2014; Zhong *et al.*, 2019)、斯里兰卡高

原(Dissanayake and Chandrajith, 1999)和印度喀拉拉邦孔兹岩带中的高级变质石墨(Radhika *et al.*, 1995)。

石墨质碳具有两个显著的特征,即低溶解度和低移动性。在俯冲带条件下,石墨质碳的溶解度远低于碳酸盐矿物的溶解度(Frost, 1979; Connolly, 1995; Caciagli and Manning, 2003; Frezzotti *et al.*, 2011),并且其移动性也低于含碳流体(Evans *et al.*, 2002),这两个特征使得石墨质碳成为俯冲带中的碳汇(carbon sink)。俯冲带中碳酸盐矿物的不稳定并

不意味着碳会离开俯冲板片而发生碳丢失,相反,在还原和低流体通量条件下,碳可以转变成相对稳定的石墨固存在板片中(Vitale Brovarone *et al.*, 2017; Tao *et al.*, 2018; Zhu *et al.*, 2020),之后随着板片折返,或者进入深部地幔作为金刚石的碳源(图2)。碳酸盐矿物在高压、低压条件下的还原反应会生成石墨和甲烷等还原性含碳相(Vitale Brovarone *et al.*, 2017; Tao *et al.*, 2018),这一反应可能会控制俯冲带中碳的赋存形式以及非生物甲烷的产量,在全球范围内量化这一进程需要进一步做更多的工作。

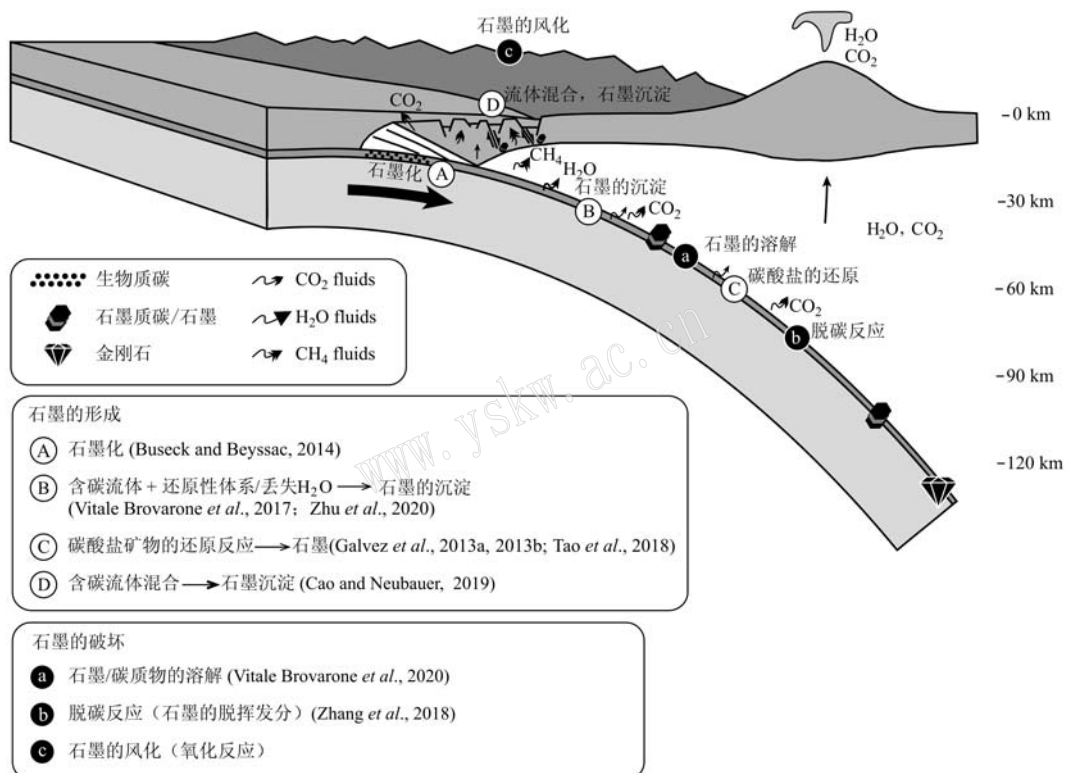


图2 俯冲带中石墨质碳循环的卡通示意图,包括石墨质碳的形成及破坏[据 Beyssac and Rumble(2014); Cao and Neubauer (2019); Tumiati *et al.* (2020)修改; A、B、C、D 和 a、b、c 放置的位置为粗略位置]

Fig. 2 Sketch illustration of the carbon cycle in subduction zones including the formation and destruction of graphitic carbon (modified after Beyssac and Rumble, 2014; Cao and Neubauer, 2019; Tumiati *et al.*, 2020; the labels A, B, C, D and a, b, c in the figure just show the general location for these reaction processes)

## 2 石墨质碳的地质循环过程

岩石圈中还原性碳主要以石墨质碳等有机碳的形式存在。岩石圈中石墨质碳的存在使其在固体地球、大气圈、水圈和生物圈之间的碳循环中起着关键作用(Berner, 2003; Beyssac and Rumble, 2014; Cao and Neubauer, 2019; Tumiati *et al.*, 2020; Galvez *et al.*, 2020)。一旦岩石中出现石墨质碳,两个主要过程会在地质时间尺度上显著影响石墨质碳的循环,进而影响全球碳循环(图2):①俯冲作用,碳在地表与地球深部之间交换;②风化侵蚀,碳在固体地球与大气圈之间交换。

在俯冲作用下,沉积物中所含石墨质碳的命运实际上是未知的。在一定的氧化还原条件下石墨质碳可以被氧化成 $\text{CO}_2$ 并溶解在流体中(图2中过程

a),然后通过火山去气作用折返到地表。此外,由于它的难溶性和热稳定性,有一部分石墨质碳可以被保存在岩石中,并俯冲进入地球深处。石墨质碳向下俯冲的循环过程可能更加复杂,除了石墨化(图2中过程A)外,俯冲过程中可能会发生无机碳储库和有机碳储库之间的交换。例如,Vitale Brovarone等(2017)和Zhu等(2020)分别在意大利阿尔卑斯地区的变质超基性岩和中国西南天山地区的变质基性岩中观察到饱和的含碳流体沉淀形成石墨(图2中过程B);Galvez等(2013a)与Tao等(2018)均在高压变质岩中观察到碳酸盐矿物还原为石墨(图2中过程C)。碳酸盐矿物的还原反应除了有石墨的生成,Vitale Brovarone等(2017)和Tao等(2018)还发现了CH<sub>4</sub>流体包裹体,这两项与非生物成因甲烷相关的研究成果,对俯冲带中无机生成油气这一变革性技术科学问题研究具有重大的指示意义。此外,在一些断裂带中,会出现富含CO<sub>2</sub>的流体与富含CH<sub>4</sub>的流体混合,从而沉淀出石墨(图2中过程D)。

当考虑到遭受风化侵蚀的岩石中石墨质碳的命运时,则会出现有机碳向无机碳转化的问题(图2中过程c)。有证据表明,石墨质碳可以抵抗原位风化,并可以长距离运输,最终在海洋沉积物中再循环(Galy et al., 2008)。相反,无序石墨质碳易被氧化(Bouchez et al., 2010),长期来看,这可能会对大气中的CO<sub>2</sub>和O<sub>2</sub>成分产生重大影响。

### 3 生成石墨质碳的途径

之前学者们认为,地球上产生石墨质碳的两个主要途径是:石墨化(graphitization)——沉积物中生物有机物质随着俯冲过程中温压的升高而通过一系列无序石墨质碳的中间阶段逐步转化为石墨(图1;Grew, 1974; Wang, 1989; Wada et al., 1994; Beyssac et al., 2002; Rahl et al., 2005; Buseck and Beyssac, 2014),以及饱和深部含碳流体在开放体系或封闭体系中沉淀出石墨(Rumble and Hoering, 1986; Farquhar and Chacko, 1991; Wopenka and Pasteris, 1993; Santosh and Wada, 1993; Luque et al., 1998; Pasteris, 1999; Evans et al., 2002; Rumble, 2014)。近些年,随着对石墨关注程度的增加,一种新的石墨形成机制——碳酸盐矿物还原生成石墨(Galvez et al., 2013a, 2013b)也逐渐被大家接受。

石墨质碳按照碳的来源可以分为有机成因(也叫生物成因)和无机成因(也叫非生物成因)。生物成因是指石墨由有机质经变质作用转变形成,石墨化形成的石墨就属于生物成因。非生物成因是指无机碳(如碳酸盐矿物、CO<sub>2</sub>等)还原生成石墨。非生物成因石墨多与变质作用相关。野外观察(Evans et al., 2002)和理论研究(Connolly, 1995)均表明非生物成因石墨可以在还原条件下形成。流体沉淀形成的石墨质碳是有机成因还是无机成因,取决于流体中碳的来源。碳酸盐矿物还原形成石墨质碳则属于无机成因。下面对这3种石墨质碳的形成机制进行详细描述。

#### 3.1 石墨质碳的石墨化过程(graphitization)

有机分子在实验室形成石墨的过程被描述为两个阶段(Oberlin, 1989):①碳化,它消除了大部分的非碳成分,并开始形成由六元平面碳环网络组成的芳香骨架,紧随其后的是②石墨化,主要是芳香族骨架向石墨热力学稳定的ABAB层序的聚合和结构重排(图1, Beyssac and Rumble, 2014)。

自然碳化和石墨化可以用Van Krevelen图来表示(图3),该图描绘了H/C与O/C原子比的演变过程。在图3中,不同的起始物质表现出不同的路径(干酪根I、II和III的分类来自Vandenbroucke and Largeau, 2007)。在该图中,石墨质碳被限制在靠近纯碳端点的狭窄区域(图3中左下角的圆点)。

大多数高级变质岩石中的石墨是通过“石墨化”得到的(图3),石墨化转变是不可逆的,是无序或部分有序的非晶体含碳物质(比石墨质碳的范围更大,指含有元素C的物质)向纯碳的结晶石墨的逐步转变,并伴随着H、O、N元素的丢失。含碳物质经历石墨化过程后,在氧逸度低、含碳流体中石墨活性高的体系中,能一直在变质岩中稳定到700℃的温度条件(Harris et al., 1993)。这种形式的碳只有经过抬升或侵蚀才能返回到地表,并且其周期远远大于CO<sub>2</sub>循环的几百万年。

#### 3.2 石墨质碳的流体沉淀机制 (fluid-deposited graphite)

石墨的流体沉淀成因涉及复杂的机制以及不同流体来源(例如地幔碳,变质脱碳反应产生的CO<sub>2</sub>,熔体脱气产生的CO<sub>2</sub>等)的不同流体种类(例如CO<sub>2</sub>、CH<sub>4</sub>、CO等)(Weis et al., 1981; Lamb and Valley, 1984; Matthey, 1987; Pineau et al., 1987; Luque et al., 1992, 1998, 2009; Farquhar et al., 1999; Satish-

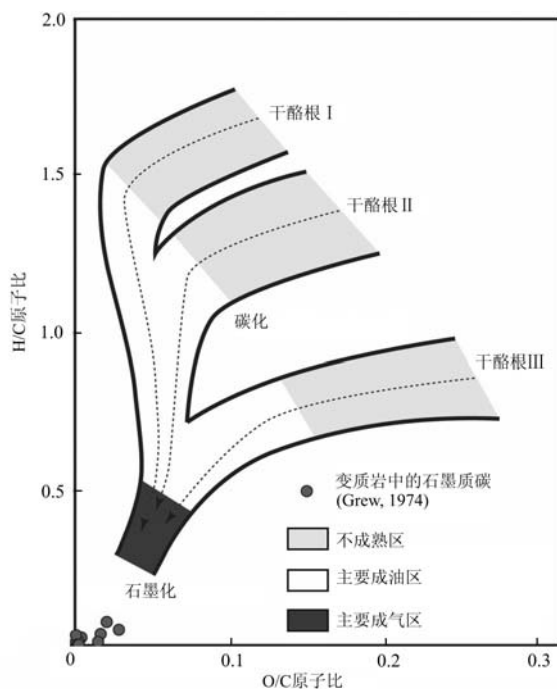


图 3 Van Krevelen 图显示了碳化过程中 3 类干酪根的化学路径以及来自选定变质岩的石墨质碳的组成数据

Fig. 3 Van Krevelen diagram showing the chemical pathways for the three classes of kerogens during carbonization and compositional data for graphitic carbon from selected metamorphic rocks

I、II 和 III 型干酪根的有机物分别主要来自湖藻、海洋微生物和陆生植物。此处, 干酪根 III 对应于煤。不成熟区代表释放大量碳氢化合物之前的条件(据 Buseck and Beyssac, 2014)

The organic matter in kerogen types I, II, and III are mainly derived, respectively, from lacustrine algae, marine microorganisms, and terrestrial plants. Here, kerogen III corresponds to coal. The immature zone represents conditions prior to the release of large amounts of hydrocarbons (after Buseck and Beyssac, 2014)

Kumar et al., 2002; Binu-lal et al., 2003)。流体沉淀生成的石墨质碳始终是高度结晶的(Pasteris, 1999), 并且系统地显示出比相同温度下石墨化生成的石墨质碳更高的结晶度(Galvez et al., 2013a)。与干酪根(干酪根是指沉积岩中不溶于碱、非氧化型酸和非极性有机溶剂的分散有机质, 主要由 C、H、O 和少量 S、N 组成, 但没有固定的分子式和结构模型)的石墨化(图 3)相比, 流体沉淀的石墨质碳一般存在于受流体-岩石强烈相互作用影响的局部地质体中, 而且通常含量很高(例如质量分数可高达全岩的 14%) (Rumble and Hoering, 1986; Luque et al., 2012, 1998; Galvez et al., 2013a; Vitale Brovarone et al., 2017); 或者被包在流体包裹体中(Cesare,

1995; Satish-Kumar, 2005; Zhu et al., 2020)。

含碳流体中石墨沉淀的机理可分为两类: ① 等化学变化(等化学条件下温度和/或压力的变化); ② 等压-等温体系的组成变化(Luque et al., 1998)。第①种机理主要依赖于 COH 流体中随着温度下降石墨稳定域的增大(Luque et al., 1998; Pasteris, 1999), 可用来解释在英国 Borrowdale 石墨矿床、南非 Stiliwater 杂岩、南非 Kaapvaal 岩石圈地幔捕掳体和俄罗斯 Siberian 克拉通等地区石墨的成因(Mathez et al., 1989; Pearson et al., 1994; Luque et al., 2009; Ortega et al., 2010)。另一方面, 通过水化反应或流体混合引起的 C-O-H 流体的化学变化被认为是导致新罕布什尔州石墨沉积物形成的主要机理(Rumble and Hoering, 1986)。

Luque 等(1998)详细讨论了流体成因石墨的特性和形成机理。当氧逸度( $f_{O_2}$ )、压力( $p$ )、温度( $t$ )、流体组成(主要种类为  $H_2O$ 、 $CO_2$ 、 $CH_4$ 、 $CO$ 、 $O_2$  和  $H_2$ )发生改变的时候, 含碳变质流体可以沉淀出石墨。C-O-H 三元图解可用来示意不同温度、压力、流体成分条件下石墨的形成(Huizenga, 2011; Huizenga and Touret, 2012)(图 4)。下面举例说明流体中石墨的形成途径:

#### (1) 等压降温

等压降温, 石墨的饱和曲线会向远离 C 端点的方向移动(图 5a), 由于流体的成分不变, 这样使得原本不饱和的流体可能会变成饱和流体, 从而沉淀出石墨。

#### (2) 流体中 $H_2O$ 含量降低

体系中含水矿物(如角闪石、绿泥石、滑石等)的形成, 导致流体丢失部分  $H_2O$ , 含碳流体会发生反应(1)来持续提供  $H_2O$  供含水矿物生长。这样流体成分会有 H 和 O 的丢失, 而没有 C 的丢失, 那么流体的成分投点便会朝向靠近端点 C 的方向移动(图 5b 中从 A 朝向 B 移动), 从而跨越石墨的饱和曲线, 导致石墨的沉淀析出。



#### (3) 两种不同成分的含碳流体混合

氧化性含碳流体渗透进入还原性含碳流体, 导致石墨的沉淀。例如富含  $CO_2$  的流体 A 和富含  $CH_4$  的流体 B 混合, 会导致混合之后的流体热力学不平衡, 混合后的流体沿着 CX 的轨迹发生反应(1), 沉淀出石墨, 直到流体达到稳定点 X(图 6; Evans et al., 2002)。相比于反应(1)(有  $H_2O$  离开

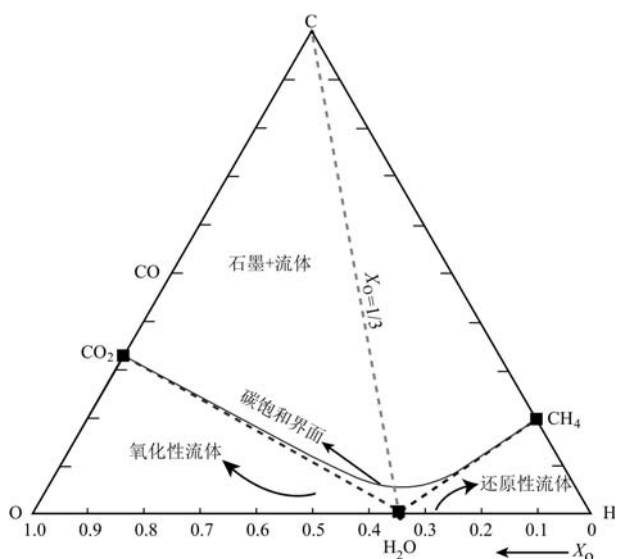


图4 C-O-H三元图显示0.5 GPa、600℃条件下包含 $\text{CO}_2$ 、 $\text{H}_2\text{O}$ 和 $\text{CH}_4$ 在内的碳的种类

Fig. 4 Ternary C-O-H diagram showing the composition of carbon species including  $\text{CO}_2$ ,  $\text{H}_2\text{O}$  and  $\text{CH}_4$  at 0.5 GPa and 600°C

黑色的曲线表示“碳饱和界面”的位置。在碳饱和界面以上,流体中的碳过饱和石墨会发生沉淀;然而,在碳饱和界面之下石墨就会被消耗掉。 $X_0$ 指示流体中O/(O+H)的原子比(据Zhang and Santosh, 2019)

The black curve indicates the position of the “carbon saturation surface”. Above the carbon saturation surface, the carbon in the fluid is supersaturated, graphite will be precipitated, while below this, the graphite will be consumed.  $X_0$ : fluid O/(O+H) atomic ratio  
(after Zhang and Santosh, 2019)

流体),富含 $\text{CO}_2$ 的流体与富含 $\text{CH}_4$ 的流体混合后,并没有 $\text{H}_2\text{O}$ 离开混合后的流体。

碳酸盐驱动的高氧逸度、富 $\text{CO}_2$ 的流体,与碳物质驱动的低氧逸度、富 $\text{CH}_4$ 的流体相混合,这种混合的流体是热力学不平衡的,可能会发生石墨的沉淀来达到平衡。这一反应机理得到了天然地质样品的验证,Evans(1998)发现钙硅酸盐和泥质岩石边界处的断层泥中有含碳物质富集,并且石墨的碳同位素值介于有机碳和碳酸盐之间(Rumble and Hoering, 1986)。如果这一反应机理在体积上是显著的,那么这对地球化学质量预算和含碳物质停留时间的估计具有重要的意义。

相比于还原性含碳流体,自然界中富含 $\text{CO}_2$ 的氧化性含碳流体沉淀形成石墨的报道更多。最初,“富含 $\text{CO}_2$ 流体沉淀形成石墨”这一猜想由Lamb等(1984)提出来。后来Santosh等(1993)对此猜想进行了验证。Santosh等(1993)对于印度Kerala Khondalite Belt的石墨进行了碳同位素研究,认为是在还原性麻粒岩中由外部来源的富含 $\text{CO}_2$ 的流体渗透而发生石墨的沉淀。该石墨具有高的碳同位素值 $\delta^{13}\text{C} = -8.6\% \sim -13.4\%$ 。此外,石墨的沉淀是由受结构控制的、同位素均一的富含 $\text{CO}_2$ 的流体渗透导致。并且石墨中保留的部分生物碳( $\delta^{13}\text{C} = -34\%$ )的特征,说明富含 $\text{CO}_2$ 的流体并不是到处渗透,只是沿着

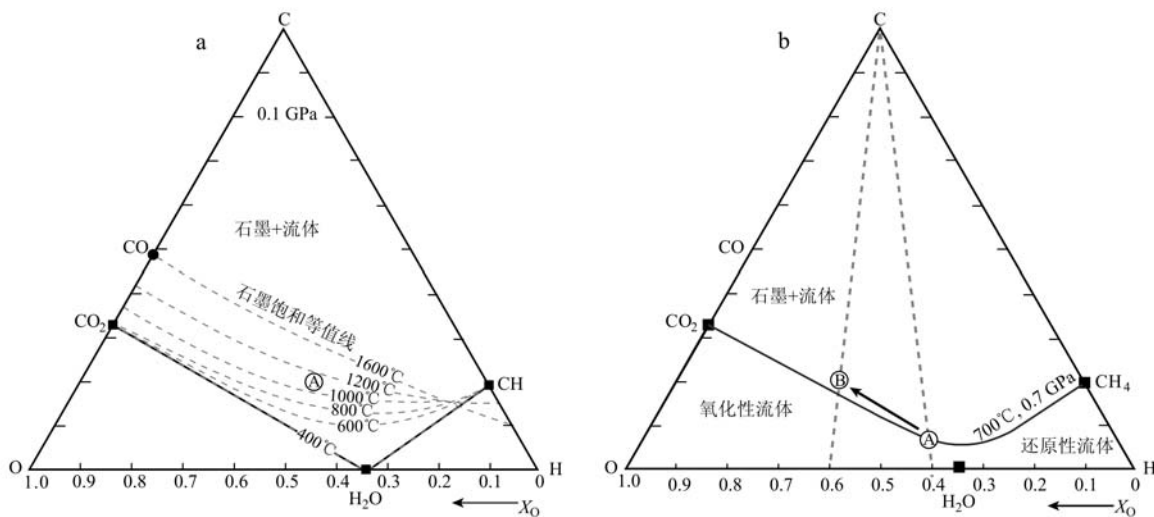


Fig. 5 Ternary C-O-H diagrams showing equilibrium-driven graphite precipitation from a fluid phase during isobaric cooling (a) and  $\text{H}_2\text{O}$  leakage (b)

a—C-O-H体系在0.1 GPa压力下显示不同温度(1 600, 1 400, 1 200, 1 000, 800, 600, 400°C)对应的石墨饱和等温线;虚线为不同温度条件对应的石墨饱和曲线(Holloway, 1984); b—C-O-H体系在700°C、0.7 GPa时候的石墨饱和等温线(van Zuilen, 2019)

a—C-O-H system at 0.1 GPa total pressure showing graphite saturation isotherms corresponding to different temperatures (1 600, 1 400, 1 200, 1 000, 800, 600, 400°C); dashed lines represent graphite saturation curves at different temperatures (after Holloway, 1984); b—C-O-H system at 700°C and 0.7 GPa showing graphite saturation isotherm (after van Zuilen, 2019)

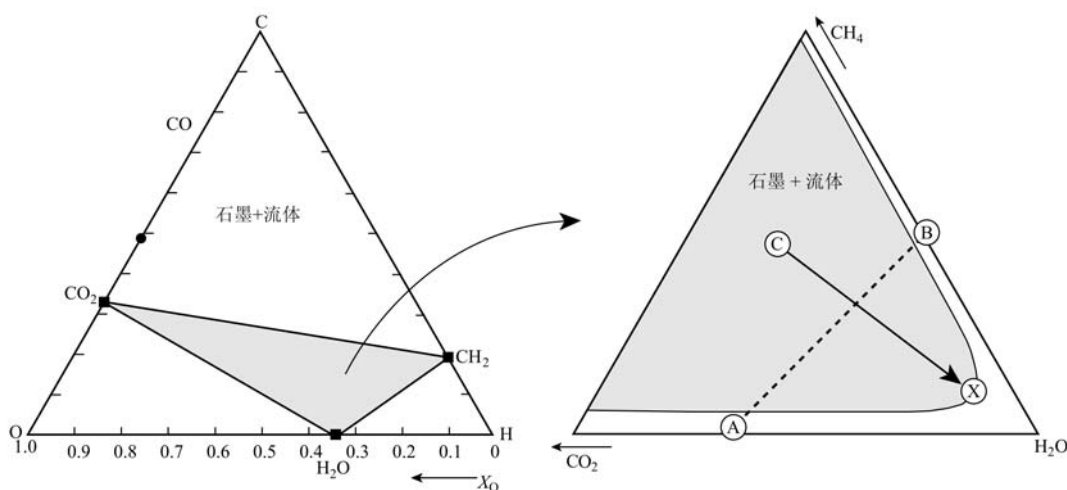
图 6 C-O-H 三元图显示  $\text{CO}_2$  流体和  $\text{CH}_4$  流体混合形成石墨

Fig. 6 Ternary C-O-H diagrams showing the formation of graphite with the mixing of  $\text{CO}_2$  fluid and  $\text{CH}_4$  fluid

C-O-H 体系显示成分分别为 A、B 的两种流体混合导致石墨的沉淀，并且混合后的流体成分会朝向稳定流体成分点 X 移动，体系的温度压力分别为  $550^\circ\text{C}$ 、0.7 GPa (Evans *et al.*, 2002)

C-O-H system shows the graphite precipitation resulting from mixing of two kinds of fluids with compositions of A and B, and the mixed fluid composition will move towards stable composition at point X. The system under  $550^\circ\text{C}$  and 0.7 GPa condition (after Evans *et al.*, 2002)

特定的通道(断裂/剪切,或者岩浆通道)渗透。Zhu 等(2020)对中国西南天山含碳酸盐榴辉岩中的石墨脉体研究表明,该石墨脉是由寄主含碳酸盐榴辉岩脱碳释放的富含  $\text{CO}_2$  的流体沉淀而形成,其中折返过程中体系温度的降低、流体中  $\text{H}_2\text{O}$  的丢失是导致 C-O-H 流体中碳饱和的关键因素。Zhang 等(2019)通过拉曼光谱和碳同位素分析确定了印度变质泥质岩中石墨的成因既有生物有机质的石墨化,同时也有地壳岩浆来源的  $\text{CO}_2$  流体的沉淀。富含  $\text{CH}_4$  的还原性流体沉淀出石墨的天然报道较少。Vitale Brovarone 等(2017)报道了意大利阿尔卑斯地区在碳酸盐化蛇纹岩中发现的石墨是由富含  $\text{CH}_4$  的流体沉淀而形成。

对于流体沉淀形成的石墨,流体碳含量的变化是控制不同石墨形态的主要因素 (Barrenechea *et al.*, 2009)。对于 Borrowdale 矿床,从中等温度的流体中沉淀出来的石墨需要很高的过饱和度 (Luque *et al.*, 2009)。根据经典的成核理论 (Walton, 1969),每单位时间在系统中形成的临界核数是过饱和度平方的指数函数。这意味着当在高过饱和条件下发生成核作用时,会形成大量较小尺寸的晶体,而在低过饱和度下发生成核作用则会形成少量较大尺寸的晶体。因此,当流体达到石墨自发成核所需的碳饱和度时,就会开始形成石墨。具有可变结晶度的缺陷

石墨晶粒的形成需要不同的动力学因子。石墨从流体中沉淀可以细分为两种沉淀模式:批次沉淀 (batch precipitation) 会生成无环带的石墨晶体;而瑞利型沉淀 (Rayleigh-type precipitation) 会形成环带明显的石墨晶体 (Farquhar and Chacko, 1991)。

### 3.3 碳酸盐矿物的还原反应 (reduction of carbonate)

野外观察 (Evans *et al.*, 2002) 和理论研究 (Connolly, 1995) 表明非生物成因石墨可以在还原条件下形成,但是这一过程的反应机制一直没有得到系统地研究。含铁碳酸盐矿物中铁元素为变价元素,可以作为缓冲剂稳定存在于较大的氧逸度条件下,因此菱铁矿和含铁白云石是研究俯冲带中碳酸盐矿物还原产生石墨的良好研究载体 (van Zuilen *et al.*, 2003; Tao *et al.*, 2014)。

碳酸盐矿物在充分还原条件下水热分解时,可以形成碳氢化合物或石墨 (Perry and Ahmad, 1977; van Zuilen *et al.*, 2002, 2003; McCollom and Seewald, 2003; Galvez *et al.*, 2013a; Milesi *et al.*, 2015)。菱铁矿 ( $\text{FeCO}_3$ ) 的水热分解导致磁铁矿 ( $\text{Fe}_3\text{O}_4$ ) 的形成,为低氧逸度创造一个直接的缓冲,这是形成石墨或有机物所必需的。Milesi 等(2015)实验表明在温度  $200$ 、 $300^\circ\text{C}$  和  $50$  MPa 的压力下,菱铁矿的水热分解生成各种溶解的有机化合物(如甲酸、乙酸、甲醇、乙醇、丙醇和丙酮)和石墨(反应式 2)。菱铁矿在水

热条件下的分解可以概括为以下一般反应(McCollom and Seewald, 2003):

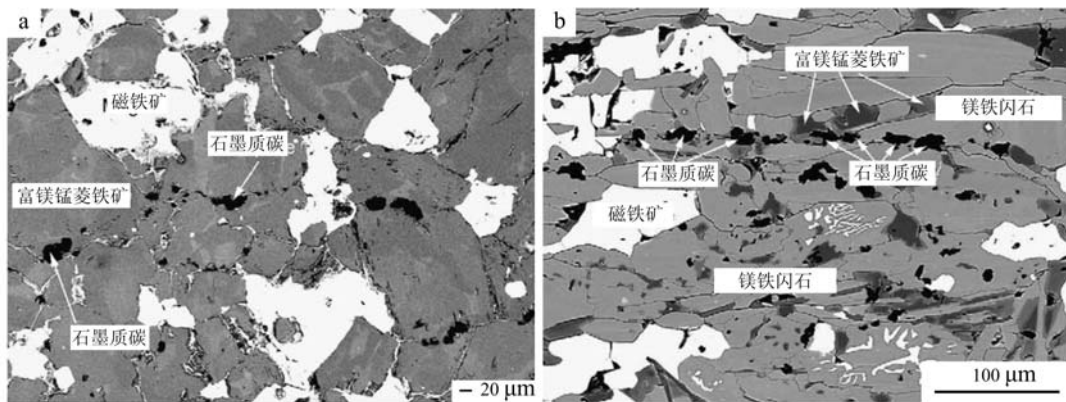
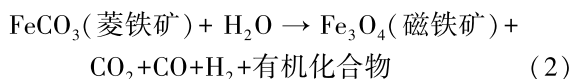
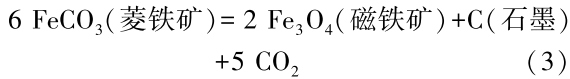


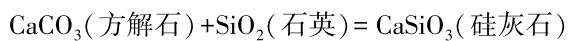
图 7 镁锰菱铁矿-磁铁矿-石墨的 SEM 照片 (van Zuilen et al., 2003)

Fig. 7 SEM images of MgMn-siderite-magnetite-graphite (after van Zuilen et al., 2003)

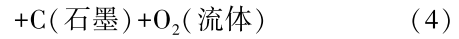


菱铁矿分解反应的实验已做了很多研究工作(有关概述请参见 van Zuilen et al., 2003),并且已知许多因素会影响菱铁矿的分解,例如阳离子组成(Mn置换Fe)、压力和系统的氧化还原状态等。

俯冲带中记录有碳酸盐矿物还原生成石墨的代表性天然岩石样品发现于阿尔卑斯科西嘉岛地区。Galvez 等(2013a)对法国科西嘉岛折返的蛇纹岩-沉积岩接触带的石墨进行了碳同位素和拉曼光谱学研究,发现高结晶度的石墨形成于俯冲变质阶段,由变质沉积岩中的方解石在蓝片岩相低温条件下( $430^{\circ}\text{C}$ ,  $0.9\sim1.5$  GPa,  $\Delta\text{QFM}=0$ )发生还原反应生成(反应式 4),其中还原性环境由超基性岩的蛇纹石化提供。接触带中石墨的碳同位素值为  $0.8\pm0.1\text{‰}$ ,与沉积岩中原始方解石的碳同位素值( $0\text{‰}$ )接近,并且石墨在结构上与同过程形成的硅灰石相关。该接触反应带的形成,是由于蛇纹岩和大理岩接触面之间在化学成分(例如 Si)上存在浓度梯度,因此扩散控制了反应的进行,形成了这样的反应带(硅灰石+石墨)(Malvoisin et al., 2012)。同时,控制反应带形成的另一个重要因素就是氧逸度,蛇纹岩和大理岩氧逸度的差别是形成 3 个不常见地质现象(方解石的还原、低温硅灰石的形成、低温石墨的形成)的重要原因。



然而,van Zuilen (2003) 对格陵兰岛 Isua Supracrustal Belt (ISB) 的古变质碳酸盐岩研究发现,菱铁矿在高于  $450^{\circ}\text{C}$  的无水变质条件下会发生分解反应形成石墨而不是有机烷烃(图 7),反应式为:



热力学计算表明,高压低温条件下,碳在 C-O-H 流体中的低溶解度是石墨沉淀同时碳酸盐失稳发生的主要原因(Galvez et al., 2013b)。因此 Galvez 等(2013a, 2013b)认为接触带中石墨的形成过程为,方解石在还原性条件下发生还原反应形成石墨质碳,而不是由沉积物中有机质碳直接通过石墨化形成石墨。这一研究结果表明,低温还原条件下方解石通过还原反应生成石墨,是俯冲带非生物成因石墨的一种形成机制,并且利于将碳运输到深部地幔。质量平衡计算表明,沉积单元中 9% 的碳质物质(原始的沉积碳 91%+非生物碳 9%)来自于反应带方解石的完全还原反应。因此,在还原条件下将碳酸盐转化为石墨可以使先前稳定存在于碳酸盐中的碳以石墨的形式稳定到俯冲带更深处。如果该过程在体积上是显著的,则氧化性碳在进入上地幔时在进变质脱挥发和熔融期间可以通过氧化性碳向还原性碳的转变来改变碳的总体稳定性。

近些年其他变质地区也有碳酸盐矿物还原成石墨的报道。Vitale Brovarone 等(2017)报道了意大利阿尔卑斯地区的碳酸盐化蛇纹岩中方解石被还原形成  $\text{CH}_4$  和还原性流体,并伴随着石墨从饱和的还原性含碳流体中沉淀。Tao 等(2018)结合天然样品和高温高压实验,确定了中国西南天山高压-超高压变质带中含碳酸盐榴辉岩中的石墨和  $\text{CH}_4$  是由含铁白云石在高压还原性条件下通过还原反应生成。因

此,除了菱铁矿外,富钙碳酸盐如方解石、白云石在俯冲带中还原性条件下也可以还原形成非生物成因的石墨甚至甲烷。

## 4 石墨质碳的水溶性

具有不同结晶度和石墨化程度的有机质是俯冲沉积物中碳的重要来源。一般认为,俯冲的含碳物质在进变质过程中大部分保留在岩石中(Cook-Kollars *et al.*, 2014)。然而,高温高压实验结果表明,包括结晶石墨在内的石墨质碳在变质条件下(如1~3 GPa, 800°C,  $\Delta\text{FMQ} \approx -0.5$ )可溶于流体中(Tumiati *et al.*, 2017, 2020),使其易于沿着渗透性通道进行流体介导的移动。这一实验结论与阿尔卑斯科西嘉岛泥质片岩中观察到的流体介导的石墨质碳的释放一致(Vitale Brovarone *et al.*, 2020)。其次,有序结晶石墨和无序碳由于其不同的热力学性质,在水溶液中表现出不同的溶解敏感性。高温高压实验岩石学证据表明,在1 GPa、800°C条件下,相比于结晶度高的石墨,无序的碳与流体反应更容易被氧化成CO<sub>2</sub>;但是在3 GPa、800°C条件下,二者与流体反应产生的CO<sub>2</sub>相差不大(Tumiati *et al.*, 2020)。换言之,俯冲带尤其是在俯冲带的浅部,当沉积物被流体交代时,相比于结晶度高的石墨,结晶度差的碳更容易释放。石墨化的动力学实验结果表明,俯冲的沉积岩中的石墨质碳在达到弧下深度(<100 km)之前,通过快速重结晶和脱挥发分变质作用完全转化为高度有序的石墨(Nakamura *et al.*, 2020; Tumiati *et al.*, 2020)。此外,高温高压实验和热力学模拟表明,当碳饱和的C-O-H流体中到达SiO<sub>2</sub>饱和时,流体中CO<sub>2</sub>的含量显著增大并伴随有机复合物的形成(Tumiati *et al.*, 2017; Tiraboschi *et al.*, 2018)。

## 5 俯冲带石墨质碳的释放

### 5.1 有机碳脱气反应脱碳

与碳酸盐的变质脱挥发分和相关的石墨沉淀(特别是在俯冲期间)相比,变质岩中的石墨质碳脱气可能也很重要,但针对这一现象开展的研究相对较少(例如Holloway, 1984; Connolly and Cesare, 1993; Cesare, 1995; Pattison, 2006; Evans *et al.*, 2008; Chu and Ague, 2013; Cook-Kollars *et al.*, 2014)。变质作用过程中,碳化阶段(图1,图3)后留

下的干酪根残渣进入石墨化阶段,在较高的温度和压力下继续释放杂原子(O、H、N、S),最终在某一时刻转化为石墨(Bernard and Papineau, 2014; Buseck and Beyssac, 2014)。在俯冲变质过程中,有机碳的质量变化和相关的碳同位素分馏可能会因一些过程而变得复杂,这些过程包括脱挥发分、封闭体系下与无机碳酸盐的碳同位素交换、氧化还原反应以及在外部衍生流体中与碳的同位素交换(Kraft and Bebout, 2017)。

变质过程中石墨的脱气作用可以产生CO<sub>2</sub>、CH<sub>4</sub>和化合物。在含石墨体系中,确切的相关关系随岩石成分、温度、压力和氧逸度而变化(Ohmoto and Kerrick, 1977; Graham *et al.*, 1983; Connolly and Cesare, 1993; Chu and Ague, 2013)。

### 5.2 石墨质碳溶解脱碳

在俯冲带中,对在封闭系统条件下变质的沉积岩的分析表明,超过75%的初始俯冲的石墨质碳可以一直保留到深度约100 km(Cook-Kollars *et al.*, 2014)。但是,俯冲的石墨质碳在开放系统条件下的行为(例如沿着流体的渗透路径)受到较少地约束。大多数关注开放体系中还原性碳行为的研究都涉及石墨的沉淀(Duke and Rumble, 1986; Evans *et al.*, 2002; Luque *et al.*, 2009; Galvez *et al.*, 2013a, 2013b; Vitale Brovarone *et al.*, 2017),而流体介导的石墨质碳释放仍然很少见(Mori *et al.*, 2014)。沿着通道化流体路径,流体-岩石的相互作用可能会强烈影响岩石中含碳相的稳定性,例如有流体参与的碳酸盐矿物的脱碳反应(Gorman *et al.*, 2006)、流体介导的碳酸盐矿物的溶解反应(Ague and Niculescu, 2014)和流体介导的岩石的固碳反应(Piccoli *et al.*, 2016, 2018)。在这种情况下,相对于封闭系统,适合石墨质碳运移的条件可能会得到改善(Tumiati *et al.*, 2017; Tumiati and Malaspina, 2019)。尽管石墨质碳在流体中的溶解度很低,但是经过长期和/或反复的渗透,流体可能逐步从含有含碳物质的岩石中去除有机碳。

Vitale Brovarone等(2020)对阿尔卑斯科西嘉岛和西阿尔卑斯的蓝片岩相俯冲杂岩的研究结果表明,在俯冲板片弧前区域高压低温条件下,泥质片岩中石墨质碳可以通过强烈的流体介导的渗透作用释放有机碳。并且,在受强烈流体渗透影响的样品中,超过90%的初始石墨质碳可以从岩石中释放。微观结构和微观拉曼数据表明,相对于接近结晶的石墨,

无序的石墨质碳更容易被选择性地从岩石中释放。这一现象与理论模拟计算和高温高压实验是一致的(Chu and Ague, 2013; Tumiati *et al.*, 2020)。在大规模流体通道化的环境中,例如沿区域尺度、岩性/构造边界或俯冲沉积堆顶部,预测俯冲的石墨质碳会发生强烈的溶解作用。因此,该过程可能会在地质时间尺度上对进入深部地幔的碳汇存在负反馈作用,并有助于从弧前区域的俯冲板片中释放具有轻同位素特征的碳。

## 6 俯冲带变质岩中石墨质碳的地质意义

除了生物有机质成因的石墨质碳,非生物成因的石墨质碳也逐渐被报道并受到越来越多的关注(Rumble and Hoering, 1986; Galvez *et al.*, 2013a; Tao *et al.*, 2018; Vitale Brovarone *et al.*, 2020; Zhu *et al.*, 2020)。碳酸盐还原和流体沉淀这两种非生物成因石墨质碳的形成机理,控制着俯冲带中无机碳向有机质石墨的转变。这种石墨质碳的出现可以有效限定流体的成分和指示氧逸度条件。石墨质碳对深层流体(Connolly and Cesare, 1993)和熔体(Cesare, 1995)的C-O-H组成起关键控制作用。一旦岩石中出现了石墨质碳,那么与该岩石平衡的流体中的碳一定是饱和的。其次,石墨质碳的碳同位素特征可用于示踪其碳的来源。碳与铁均是变价元素,是俯冲带氧化还原条件的主要缓冲剂之一。石墨也与诸如单质硫、碳酸盐和粘土之类的矿物相互作用,并有助于控制氧化还原条件。这种石墨质碳具有复杂的变质演化过程,它可能受控于物理变化(如流体流动和变形等)和地球化学改变(如体系的氧逸度改变)(Vitale Brovarone *et al.*, 2020)。除了上述作用,石墨质碳可以作为俯冲带蛇纹岩中非生物成因甲烷的碳源(Vitale Brovarone *et al.*, 2017)。

## 7 结语

(1) 俯冲带中石墨质碳的碳质来源有生物有机质、有机或无机来源的含碳流体以及无机碳酸盐矿物。俯冲作用和风化侵蚀是石墨质碳全球循环的两个主要过程。其中俯冲作用对石墨质碳的地球内部循环影响较大。

(2) 俯冲带中石墨质碳的成因机制主要有3种:生物有机质石墨化(有机成因)、饱和含碳流体沉

淀(既有有机成因也有无机成因,取决于流体中碳的来源)、碳酸盐矿物的还原反应(无机成因)。

(3) 流体沉淀石墨的机理分为3种:等化学体系的降温来改变石墨的饱和曲面、含碳流体丢失水从而使含碳流体达到碳饱和、两种成分的流体混合形成了碳饱和的流体。

(4) 俯冲带中石墨质碳可通过脱气和溶解的方式释放。

**致谢** 诚挚感谢两位评审专家严谨细致的审阅全文,并提出很多建设性修改意见和建议,对论文质量的提高很有帮助。

## References

- Ague J J and Niculescu S. 2014. Carbon dioxide released from subduction zones by fluid-mediated reactions[J]. *Nature Geoscience*, 7: 355~360.
- Barrenechea J F, Luque F J, Millward D, *et al.* 2009. Graphite morphologies from the Borrowdale deposit (NW England, UK): Raman and SIMS data[J]. *Contributions to Mineralogy and Petrology*, 158: 37~51.
- Berglund L and Touret J. 1976. Garnet-biotite gneiss in system du graphite (Madagascar): Petrology and fluid inclusions[J]. *Lithos*, 9(2): 139~148.
- Bernard S and Papineau D. 2014. Graphitic carbons and biosignatures [J]. *Elements*, 10(6): 435~440.
- Berner R A. 2003. The long-term carbon cycle, fossil fuels and atmospheric composition[J]. *Nature*, 426: 323~326.
- Beyssac O and Rumble D. 2014. Graphitic carbon: A ubiquitous, diverse, and useful geomaterial[J]. *Elements*, 10(6): 415~420.
- Beyssac O, Rouzaud J, Goffé B, *et al.* 2002. Graphitization in a high-pressure, low-temperature metamorphic gradient: A Raman microspectroscopy and HRTEM study[J]. *Contributions to Mineralogy and Petrology*, 143: 19~31.
- Binulal S S, Kehelpannala K V W, Satish-Kumar M, *et al.* 2003. Multi-stage graphite precipitation through protracted fluid flow in sheared metagranitoid, Digana, Sri Lanka: Evidence from stable isotopes [J]. *Chemical Geology*, 197(1): 253~270.
- Black P M. 1977. Regional high pressure metamorphism in New Caledonia: Phase equilibria in the Ouegoa District[J]. *Tectonophysics*, 43(1~2): 89~107.

- Bouchez J, Beyssac O, Galy V, et al. 2010. Oxidation of petrogenic organic carbon in the Amazon floodplain as a source of atmospheric CO<sub>2</sub>[J]. *Geology*, 38(3): 255~258.
- Buseck P R and Beyssac O. 2014. From organic matter to graphite: Graphitization[J]. *Elements*, 10(6): 421~426.
- Caciagli N C and Manning C E. 2003. The solubility of calcite in water at 6~16 kbar and 500~800°C [J]. *Contributions to Mineralogy and Petrology*, 146: 275~285.
- Cao S Y and Neubauer F. 2019. Graphitic material in fault zones: Implications for fault strength and carbon cycle [J]. *Earth-Science Reviews*, 194: 109~124.
- Cesare B. 1995. Graphite precipitation in C-O-H fluid inclusions: Closed system compositional and density changes, and thermobarometric implications[J]. *Contributions to Mineralogy and Petrology*, 122(1): 25~33.
- Chu X and Ague J J. 2013. Phase equilibria for graphitic metapelite including solution of CO<sub>2</sub> in melt and cordierite: Implications for dehydration, partial melting and graphite precipitation[J]. *Journal of Metamorphic Geology*, 31(8): 843~862.
- Connolly J. 1995. Phase diagram methods for graphitic rocks and application to the system C-O-H-FeO-TiO<sub>2</sub>-SiO<sub>2</sub>[J]. *Contributions to Mineralogy and Petrology*, 119(1): 94~116.
- Connolly J and Cesare B. 1993. C-O-H-S fluid composition and oxygen fugacity in graphitic metapelites[J]. *Journal of Metamorphic Geology*, 11(3): 379~388.
- Cook-Kollars J, Bebout G E, Collins N C, et al. 2014. Subduction zone metamorphic pathway for deep carbon cycling: I. Evidence from HP/UHP metasedimentary rocks, Italian Alps[J]. *Chemical Geology*, 386: 31~48.
- Diessel C F K and Offler R. 1975. Change in physical properties of coalified and graphitised phytoclasts with grade of metamorphism [J]. *Neues Jahrbuch für Mineralogie-Monatshefte*, 1(1): 11~26.
- Dissanayake C B and Chandrajith R. 1999. Sri Lanka-Madagascar Gondwana linkage: Evidence for a Pan-African mineral belt[J]. *Journal of Geology*, 107(2): 223~235.
- Duke E F and Rumble D. 1986. Textural and isotopic variations in graphite from plutonic rocks, South-Central New Hampshire[J]. *Contributions to Mineralogy and Petrology*, 93(4): 409~419.
- Duncan M S and Dasgupta R. 2017. Rise of Earth's atmospheric oxygen controlled by efficient subduction of organic carbon[J]. *Nature Geoscience*, 10(5): 387~392.
- Evans K A, Bickle M J, Skelton D L, et al. 2002. Reductive deposition of graphite at lithological margins in East Central Vermont: A Sr, C and O isotope study[J]. *Journal of Metamorphic Geology*, 20(8): 781~798.
- Evans K A. 1998. Acadian Metamorphic Fluid Flow in East Central Vermont[D]. University of Cambridge, Cambridge, England.
- Evans M J, Derry L A and France-Lanord C. 2008. Degassing of metamorphic carbon dioxide from the Nepal Himalaya[J]. *Geochemistry Geophysics Geosystems*, 9(4): Q04021.
- Facq S, Daniel I, Montagnac G, et al. 2014. In situ Raman study and thermodynamic model of aqueous carbonate speciation in equilibrium with aragonite under subduction zone conditions[J]. *Geochimica et Cosmochimica Acta*, 132: 375~390.
- Farquhar J and Chacko T. 1991. Isotopic evidence for involvement of CO<sub>2</sub>-bearing magmas in granulite formation[J]. *Nature*, 354: 60~63.
- Farquhar J, Hauri E and Wang J. 1999. New insights into carbon fluid chemistry and graphite precipitation: SIMS analysis of granulite facies graphite from Ponmudi, South India [J]. *Earth and Planetary Science Letters*, 171(4): 607~621.
- Franklin R E. 1951. Crystallite growth in graphitizing and non-graphitizing carbons[J]. *Proceedings of the Royal Society of London Series*, 209(1 097): 196~218.
- Frezzotti M L, Selverstone J, Sharp Z D, et al. 2011. Carbonate dissolution during subduction revealed by diamond-bearing rocks from the Alps[J]. *Nature Geoscience*, 4: 703~706.
- Frost B R. 1979. Mineral equilibria involving mixed-volatiles in a C-O-H fluid phase: The stabilities of graphite and siderite[J]. *American Journal of Science*, 279(9): 1 033~1 059.
- Galvez M E, Beyssac O, Martinez I, et al. 2013a. Graphite formation by carbonate reduction during subduction[J]. *Nature Geoscience*, 6: 473~477.
- Galvez M E, Fischer W, Jaccard S, et al. 2020. Materials and pathway of the organic carbon cycle through time[J]. *Nature Geoscience*, 13(8): 535~546.
- Galvez M E, Martinez I, Beyssac O, et al. 2013b. Metasomatism and graphite formation at a lithological interface in Malaspina (Alpine Corsica, France)[J]. *Contributions to Mineralogy and Petrology*, 166: 1 687~1 708.
- Galy V, Beyssac O, France-Lanord C, et al. 2008. Recycling of graphite during Himalayan erosion: A geological stabilization of carbon in the crust[J]. *Science*, 322(5 903): 943~945.
- Gorman P J, Kerrick D M and Connolly J A D. 2006. Modelling open system metamorphic decarbonation of subducting slabs[J]. *Geochemistry Geophysics Geosystems*, 7(4): Q04007.

- Graham C M, Greig K M, Sheppard S M P, et al. 1983. Genesis and mobility of the H<sub>2</sub>O-CO<sub>2</sub> fluid phase during regional greenschist and epidote amphibolite facies metamorphism: A petrological and stable isotope study in the Scottish Dalradian[J]. *Journal of the Geological Society*, 140(4): 577~599.
- Grew E S. 1974. Carbonaceous material in some metamorphic rocks of New England and other areas[J]. *The Journal of Geology*, 82(1): 50~73.
- Harris N B W, Jackson D H, Matthey D P, et al. 1993. Carbon-isotope constraints on fluid advection during contrasting examples of incipient Charnockite formation[J]. *Journal of Metamorphic Geology*, 11: 833~843.
- Hayes J M and Waldbauer J R. 2006. The carbon cycle and associated redox processes through time[J]. *Philosophical Transactions of the Royal Society B: Biological Sciences*, 361(1 470): 931~950.
- Hermann J, Spandler C, Hack A, et al. 2006. Aqueous fluids and hydrous melts in high-pressure and ultra-high pressure rocks: Implications for element transfer in subduction zones[J]. *Lithos*, 92(3~4): 399~417.
- Holloway J R. 1984. Graphite-CH<sub>4</sub>-H<sub>2</sub>O-CO<sub>2</sub> equilibria at low-grade metamorphic conditions[J]. *Geology*, 12(8): 455~458.
- Huijzen J M. 2011. Thermodynamic modelling of a cooling C-O-H fluid-graphite system: Implications for hydrothermal graphite precipitation [J]. *Mineralium Deposita*, 46(1): 23~33.
- Huijzen J M and Touret J L R. 2012. Granulites, CO<sub>2</sub> and graphite[J]. *Gondwana Research*, 22 (3~4): 799~809.
- Kelemen P B and Manning C E. 2015. Reevaluating carbon fluxes in subduction zones, what goes down, mostly comes up[J]. *Proceedings of the National Academy of Sciences of the United States of America*, 112: 3 997~4 006.
- Kraft K and Bebout G E. 2017. Fate of Subducting Organic Carbon: Evidence From HP/UHP Metasedimentary Suites[M]. AGU Fall Meeting. Abstract 31.
- Lamb W and Valley J W. 1984. Metamorphism of reduced granulites in low CO<sub>2</sub> vapour free environments[J]. *Nature*, 312: 56~58.
- Landis C A. 1971. Graphitization of dispersed carbonaceous materials in metamorphic rocks[J]. *Contributions to Mineralogy and Petrology*, 30: 34~45.
- Luque F J, Crespo-Feo E, Barrenechea J F, et al. 2012. Carbon isotopes of graphite: Implications on fluid history[J]. *Geoscience Frontiers*, 3(2): 197~207.
- Luque F J, Ortega L, Barrenechea J, et al. 2009. Deposition of highly crystalline graphite from moderate temperature fluids[J]. *Geology*, 37(3): 275~278.
- Luque F J, Pasteris J D, Wopenka B, et al. 1998. Natural fluid-deposited graphite: Mineralogical characteristics and mechanisms of formation[J]. *American Journal of Science*, 298: 471~498.
- Luque F J, Rodas M and Galán E. 1992. Graphite vein mineralization in the ultramafic rocks of southern Spain: Mineralogy and genetic relationships[J]. *Mineralium Deposita*, 27: 226~233.
- Malvoisin B, Chopin C, Brunet F, et al. 2012. Low-temperature wollastonite formed by carbonate reduction: A marker of serpentinite redox conditions[J]. *Journal of Petrology*, 53(1): 159~176.
- Mathez E A, Dietrich V J, Holloway J R, et al. 1989. Carbon distribution in the stillwater complex and evolution of vapor during crystallization of stillwater and bushveld magmas[J]. *Journal of Petrology*, 30(1): 153~173.
- Matthey D P. 1987. Carbon isotopes in the mantle[J]. *Terra Cognita*, 7: 31~37.
- McCollom T M and Seewald J S. 2003. Experimental constraints on the hydrothermal reactivity of organic acids and acid anions: I. Formic acid and formate[J]. *Geochimica et Cosmochimica Acta*, 67(19): 3 625~3 644.
- Milesi V, Guyot F, Brunet F, et al. 2015. Formation of CO<sub>2</sub>, H<sub>2</sub> and condensed carbon from siderite dissolution in the 200~300°C range and at 50 MPa[J]. *Geochimica et Cosmochimica Acta*, 154: 201~211.
- Miyashiro A. 1964. Oxidation and reduction in the Earth's crust with special reference to the role of graphite[J]. *Geochimica et Cosmochimica Acta*, 28: 717~729.
- Mori Y, Shigeno M and Nishiyama T. 2014. Fluid-metapelitic interaction in an ultramafic melange: Implications for mass transfer along the slab-mantle interface in subduction zones[J]. *Earth, Planets and Space*, 66(1): 1~8.
- Mullis J, Dubessy J, Poty B, et al. 1994. Fluid regimes during late stages of a continental collision: Physical, chemical, and stable isotope measurements of fluid inclusions in fissure quartz from a geotraverse through the Central Alps, Switzerland[J]. *Chemical Geology*, 58 (10): 2 239~2 267.
- Nakamura Y, Yoshino T and Satish-Kumar M. 2020. Pressure dependence of graphitization: Implications for rapid recrystallization of carbonaceous material in a subduction zone[J]. *Contributions to Mineralogy and Petrology*, 175(4): 32.
- Oberlin A. 1989. High-resolution TEM studies of carbonization and graphitization[A]. Thrower P A. *Chemistry and Physics of Carbon* 22[C]. Marcel Dekker, New York, 1~143.

- Ohmoto H and Kerrick D. 1977. Devolatilization equilibria in graphitic systems[J]. *American Journal of Science*, 277(8): 1 013~1 044.
- Ortega L, Millward D, Luque F J, et al. 2010. The graphite deposit at Borrowdale (UK): A catastrophic mineralizing event associated with Ordovician magmatism[J]. *Geochimica et Cosmochimica Acta*, 74: 2 429~2 449.
- Pasteris J D. 1999. Causes of the uniformly high crystallinity of graphite in large epigenetic deposits[J]. *Journal of Metamorphic Geology*, 17 (6): 779~787.
- Pattison D R M. 2006. The fate of graphite in prograde metamorphism of pelites: An example from the Ballachulish aureole, Scotland[J]. *Lithos*, 88: 85~89.
- Pearson D G, Boyd F R, Haggerty S E, et al. 1994. The characterisation and origin of graphite in cratonic lithospheric mantle: a petrological carbon isotope and Raman spectroscopy study[J]. *Contributions to Mineralogy and Petrology*, 115(4): 449~466.
- Perry E C and Ahmad S N. 1977. Carbon isotope composition of graphite and carbonate minerals from 3. 8-AE metamorphosed sediments, Isuakasia, Greenland[J]. *Earth and Planetary Science Letters*, 36 (2): 280~284.
- Piccoli F, Vitale Brovarone A, Beyssac O, et al. 2016. Carbonation by fluid-rock interactions at high-pressure conditions: Implications for carbon cycling in subduction zones[J]. *Earth and Planetary Science Letters*, 445: 146~159.
- Piccoli F, Brovarone A V and Ague J J. 2018. Field and petrological study of metasomatism and high-pressure carbonation from lawsonite eclogite-facies terrains, Alpine Corsica[J]. *Lithos*, 304: 16~37.
- Pineau F, Javoy M and Kornprobst J. 1987. Primary igneous graphite in ultramafic xenoliths: II. Isotopic composition of the carbonaceous phases present in xenoliths and host lava at Tissemt (Algerian Sahara)[J]. *Journal of Petrology*, 28(2): 313~322.
- Plank T. 2014. Treatise on Geochemistry [M]. Second Edition Elsevier, Oxford, 203 ~ 247.
- Poli S. 2015. Carbon mobilized at shallow depths in subduction zones by carbonatitic liquids[J]. *Nature Geoscience*, 8: 633~636.
- Radhika U P, Santosh M and Wada H. 1995. Graphite occurrences in southern Kerala: Characteristics and genesis [J]. *Journal of the Geological Society of India*, 45(6): 653~666.
- Rahl J M, Anderson K M, Brandon M T, et al. 2005. Raman spectroscopic carbonaceous material thermometry of low-grade metamorphic rocks: Calibration and application to tectonic exhumation in Crete, Greece[J]. *Earth and Planetary Science Letters*, 240(2): 339~354.
- Rumble D. 2014. Hydrothermal graphitic carbon[J]. *Elements*, 10(6): 427~433.
- Rumble D and Hoering T C. 1986. Carbon isotopic geochemistry of graphite vein deposits from New Hampshire, USA [J]. *Geochimica et Cosmochimica Acta*, 50(6): 1 239~1 247.
- Santosh M and Wada H. 1993. A carbon isotope study of graphites from the Kerala Khondalite Belt, Southern India: Evidence for CO<sub>2</sub> infiltration in granulites[J]. *The Journal of Geology*, 101(5): 643~651.
- Satish-Kumar M. 2005. Graphite-bearing CO<sub>2</sub>-fluid inclusions in granulites: Insights on graphite precipitation and carbon isotope evolution [J]. *Geochimica et Cosmochimica Acta*, 69(15): 3 841~3 856.
- Satish-Kumar M, Wada H and Santosh M. 2002. Constraints on the application of carbon isotope thermometry in high- to ultrahigh-temperature metamorphic terranes[J]. *Journal of Metamorphic Geology*, 20(3): 335~350.
- Tao R B, Zhang L F, Fei Y W, et al. 2014. The effect of Fe on the stability of dolomite at high pressure: Experimental study and petrological observation in eclogite from southwestern Tianshan, China[J]. *Geochimica et Cosmochimica Acta*, 143: 253~267.
- Tao R B, Zhang L F, Tian M, et al. 2018. Formation of abiotic hydrocarbon from reduction of carbonate in subduction zones: Constraints from petrological observation and experimental simulation [J]. *Geochimica et Cosmochimica Acta*, 239: 390~408.
- Tarantola A, Mullis J, Vennemann T, et al. 2007. Oxidation of methane at the CH<sub>4</sub>/H<sub>2</sub>O-(CO<sub>2</sub>) transition zone in the external part of the Central Alps, Switzerland: Evidence from stable isotope investigations[J]. *Chemical Geology*, 237(3): 329~357.
- Tiraboschi C, Tumiati S, Sverjensky D, et al. 2018. Experimental determination of magnesia and silica solubilities in graphite-saturated and redox-buffered high-pressure COH fluids in equilibrium with forsterite+enstatite and magnesite+enstatite[J]. *Contributions to Mineralogy and Petrology*, 173(1): 2.
- Tumiati S and Malaspina N. 2019. Redox processes and the role of carbon-bearing volatiles from the slab-mantle interface to the mantle wedge[J]. *Journal of the Geological Society*, 176(2): 388~397.
- Tumiati S, Tiraboschi C, Miozzi F, et al. 2020. Dissolution susceptibility of glass-like carbon versus crystalline graphite in high-pressure aqueous fluids and implications for the behavior of organic matter in subduction zones[J]. *Geochimica et Cosmochimica Acta*, 273: 383~402.
- Tumiati S, Tiraboschi C, Sverjensky D A, et al. 2017. Silicate dissolution boosts the CO<sub>2</sub> concentrations in subduction fluids[J]. *Nature*

- Communications, 8: 616.
- Vandenbroucke M and Largeau C. 2007. Kerogen origin, evolution and structure[J]. *Organic Geochemistry*, 38: 719~833.
- van Zuilen M A, Lepland A and Arrhenius G. 2002. Reassessing the evidence for the earliest traces of life[J]. *Nature*, 418: 627~630.
- van Zuilen M A, Lepland A, Teranes J, et al. 2003. Graphite and carbonates in the 3.8 Ga old Isua Supracrustal Belt, southern West Greenland[J]. *Precambrian Research*, 126(3): 331~348.
- van Zuilen M A. 2019. Earth's Oldest Rocks[M]. Elsevier, 945~963.
- Vitale Brovarone A, Martinez I, Elmaleh A, et al. 2017. Massive production of abiotic methane during subduction evidenced in metamorphosed ophicarbonates from the Italian Alps[J]. *Nature Communications*, 8: 14 134.
- Vitale Brovarone A, Tumiati S, Piccoli F, et al. 2020. Fluid-mediated selective dissolution of subducting carbonaceous material: Implications for carbon recycling and fluid fluxes at forearc depths[J]. *Chemical Geology*, 549: 119 682.
- Wada H, Tomita T, Matsuura K, et al. 1994. Graphitization of carbonaceous matter during metamorphism with references to carbonate and pelitic rocks of contact and regional metamorphisms, Japan [J]. *Contributions to Mineralogy and Petrology*, 118(3): 217~228.
- Walton A G. 1969. Nucleation in liquids and solutions[A]. Zettlemoyer A C. *Nucleation*[C]. Elsevier, 225~307.
- Wang A, Dhamelincourt P, Dubessy J, et al. 1989. Characterization of graphite alteration in an uranium deposit by micro-Raman spectroscopy, X-RAY diffraction, Transmission Electron Microscopy and Scanning Electron Microscopy[J]. *Carbon*, 27(2): 209~218.
- Weis P, Friedman I and Gleason J P. 1981. The origin of epigenetic graphite: Evidence from isotopes[J]. *Geochimica et Cosmochimica Acta*, 45: 2 325~2 332.
- Wopenka B and Pasteris J D. 1993. Structural characterization of kerogens to granulite-facies graphite: Applicability of Raman microprobe spectroscopy[J]. *American Mineralogist*, 78(5): 533~557.
- Yang Q Y, Santosh M and Wada H. 2014. Graphite mineralization in Paleoproterozoic khondalites of the North China Craton: A carbon isotope study[J]. *Precambrian Research*, 255: 641~652.
- Zhang C and Santosh M. 2019. Coupled laser Raman spectroscopy and carbon stable isotopes of graphite from the khondalite belt of Kerala, southern India[J]. *Lithos*, 334~335: 245~253.
- Zhang S, Ague J J and Vitale Brovarone A. 2018. Degassing of organic carbon during regional metamorphism of pelites, Wepawaug Schist, Connecticut, USA[J]. *Chemical Geology*, 490: 30~44.
- Zhong Y, Ma X, Li H, et al. 2019. Revisit and comparative analysis of the typical graphite deposits in the Paleoproterozoic khondalite series, western North China Craton: Implications for genesis, depositional environment and prospecting Potential [J]. *Ore Geology Reviews*, 109: 370~380.
- Zhu J J, Zhang L F, Tao R B, et al. 2020. The formation of graphite-rich eclogite vein in SW Tianshan (China) and its implication for deep carbon cycling in subduction zone[J]. *Chemical Geology*, 533: 119 430.